The magnetocaloric performance in pure and mixed magnetic phase CoMnSi

K Morrison, A Barcza, Jd Moore, Kg Sandeman, Mk Chattopadhyay, Sb Roy, Ad Caplin, Lf Cohen

The magnetocaloric performance in pure and mixed magnetic phase CoMnSi

K Morrison[1], A Barcza[2], JD Moore[1], KG Sandeman[2], MK Chattopadhyay[3], SB Roy[3], AD Caplin[1] and LF Cohen[1]

[1]*The Blackett Laboratory, Imperial College, London SW7 2BZ, UK*

[2]*Department of Material Science and Metallurgy, University of Cambridge, Cambridge CB2 3QZ, UK*

[3] *Magnetic and Superconducting Materials section, Raja Ramanna Centre for Advanced Technology, Indore 452013, India*

Abstract

Here we study the influence of sample preparation on the magnetocaloric properties of CoMnSi. Slow cooling from the high temperature hexagonal phase of the melt to the room temperature orthorhombic phase encourages the formation of a homogenous material with large entropy changes when the system undergoes a coincident first order structural and (meta)magnetic transition. Samples that were quenched directly after annealing show a compressed *a* axis lattice parameter. Hall probe imaging indicates that the quenched sample has spatially inhomogeneous magnetic properties, which we attribute to strain because within error neither XRD nor EDX indicates a second compositional phase. Calorimetric methods and global magnetization are used to examine the entropy changes of the pure and mixed magnetic phase compounds and we make a direct comparison of these materials in terms of their refrigerant capacity.

PACS: 75.30.Sg, 75.30.Kz & 75.50.Ee

1. Introduction

The magnetocaloric effect manifests as a change in temperature of a material as it is driven through a magnetic transition by an externally applied magnetic field. Recent interest in this phenomenon is aimed toward application in room temperature refrigeration,[1] where increased efficiency and a reduction of the environmentally harmful effects associated with the traditional CFC refrigeration system could be possible.

To compare the magneto-thermal properties of candidate refrigerants there are a variety of parameters that are usually measured, the isothermal entropy change with field, ΔS, adiabatic temperature change, ΔT_{ad}, (which can be obtained directly or indirectly from magnetization and calorimetry data)[2] and the refrigerant capacity, q, (which can be determined from the isothermal entropy change as a function of temperature).[3,4,5] Difficulty lies in the comparison of these quantities to determine the *better* refrigerant when the group of materials of interest show widely varying working temperatures, peak entropy changes and levels of hysteretic losses.

The discovery of the giant and colossal magnetocaloric effect (GMCE, CMCE)[6,7] instigated the search for materials that exhibit a first order phase transition on application of a magnetic field. Although these systems as a rule show some form of hysteresis, which is detrimental to the efficiency of a cooling cycle, (and usually associated with a first order phase transition), the large entropy changes associated with them are encouraging for application. For many of the 'giant' and 'colossal' magnetocaloric materials the origin of such large entropy changes is the coupling or coincidence of a magnetic and structural transition that can add either advantageously[8] or in opposition.[9,10] To improve the performance of materials which exhibit first order behaviour in terms of tuning the accompanying hysteresis, various methods have been successfully applied to some potential refrigerants, such as doping with Fe[5] and melt-spinning.[11] Despite these advances, most reported prototypes for magnetic refrigeration use Gd,[12] a second order material, with (by

definition) a continuous phase transition, no hysteresis and an entropy change in magnetic field distributed across a wide temperature span.

The main question that we wish to address here is whether samples that are of mixed magnetic phase, by which we mean that they contain both first order and second order magnetic behaviour, may offer some advantage for application in terms of reduced hysteresis, increased temperature range of operation, or enhanced isothermal entropy change. Here we study two differently prepared samples of CoMnSi, an inverse[13] magnetocaloric material that exhibits an antiferromagnetic (AFM) to ferromagnetic (FM) field-driven phase transition.[14,15,16]

The high sensitivity of first order magnetocaloric materials to strain is a potentially useful tool for tuning the magnetocaloric effect. In the particular case of CoMnSi the sensitivity of magnetism to strain is due to the known high magneto-elastic interaction.[17] However, such a property must be carefully managed as machining can often introduce uncontrolled strain, or indeed can heat a material and take it through its magnetoelastic transition, resulting in a change of shape. These issues are part of the wider investigation into the viability of these materials for application. For example, in the case of sintered La-Fe-Si, thermal decomposition processes are being used to control the shape.[18] There are no reported studies into these issues, to the best of our knowledge, for the CoMnSi system.

The magnetic phase transition in the CoMnSi system is highly sensitive to the separation of Mn atoms in the lattice resulting in it being responsive to annealing routes (homogenous stoichiometry) and post-annealing cooling treatment.[14,16,19] By allowing the sample to cool slowly at a rate of approximately 0.2K/min, the change from high temperature hexagonal phase to low temperature orthorhombic phase ($T_{orth\text{-}hex}$~1200K)[15] is completed and the system equilibrates to its lowest energy state. In contrast rapid cooling by quenching leaves the material in an

unrelaxed strained state with a degree of lattice distortion. Scanning electron microscopy and energy dispersive X-Ray Analysis (EDX) measurements are used to confirm that both samples have similar stoichiometry. No spatial variation in the stoichiometry was detected across either sample using EDX and no second phase component was detected to within 5% accuracy of XRD. The quenched sample shows mixed magnetic character with regions showing sharp first order hysteretic behaviour and regions which show continuous phase transitions. The combination of magnetic phase transitions is confirmed by latent heat and calorimetry measurements. Hall probe imaging is used to construct a map to illustrate this distribution of properties. The refrigerant capacity of the mixed magnetic phase sample and the pure sample is compared.

2. Experimental

The samples studied here were prepared by induction melting stoichiometric amounts. The first, labelled for simplicity as $CoMnSi_{SC}$, was annealed at 950°C for 60 hours, then slow-cooled at a rate of approximately 0.2K/min. The second, $CoMnSi_{Q}$, was similarly annealed before being quenched in water at room temperature.

Magnetization measurements were carried out in an Oxford instruments VSM capable of reaching fields ±4T and temperatures ranging from 4.2-295K. For Hall imaging, a Hall probe with active area $5\mu m^2$ was scanned across the sample surface and the corresponding Hall voltage, V_H, at each point measured. Further details of this method can be found elsewhere.[20] A flat surface was prepared by polishing with varying grades of diamond paste.

Latent heat and ac calorimetry measurements were performed on approximately 100x100x50μm (~$100\mu m^3$) sized fragments using a microcalorimeter in a continuous flow cryostat with an 8T magnetic field.[21,22] To calculate the entropy change of the fragment due to latent heat (ΔS_{LH}) and

change in heat capacity (ΔS_{HC}), equations (1) & (2) are used, where ΔQ_L is the heat output due to latent heat at temperature T and C(H,T) is the heat capacity in magnetic field H (chosen here as 8T) at temperature T. The reference temperature, T1, used in the integral of Eq. (2) is chosen as a point where the entropy change is well-defined (normally zero) measured from bulk magnetization. Further details of the experimental techniques used are given elsewhere.[10,22,23] The total, ΔS_{total} ($=\Delta S_{HC}+\Delta S_{LH}$), can be compared to the entropy calculated from bulk samples[23] using the Maxwell relation given in equation (3),[24] although we should add that care needs to be taken when using the Maxwell relation in first order materials.[25]

$$\Delta S_{LH} = -\frac{\Delta Q_L}{T} \qquad (1)$$

$$\Delta S_{HC} = \int_{T1}^{T} \frac{(C(H,T) - C(0,T))dT}{T} \qquad (2)$$

$$\Delta S_M = \int_{H_1}^{H_2} \left(\frac{\partial M}{\partial T} \right)_H dH \qquad (3)$$

3. Results

3.1. X-Ray Diffraction (XRD)

X-ray powder diffraction and Rietveld refinement using an internal Si standard yielded a good fit to a single phase (to within 5% error), orthorhombic *Pnma* structure in both the $CoMnSi_{SC}$ and $CoMnSi_Q$ samples.[16] The lattice parameters are summarized in Table 1 alongside typical lattice parameters of the hexagonal and orthorhombic phase of CoMnSi as measured by Johnson.[26] Notice that the *b* and *c* lattice parameters are similar in each sample (within error ± 0.005Å) but that *a* is significantly smaller in $CoMnSi_Q$ compared to $CoMnSi_{SC}$. As the material moves from a high temperature hexagonal to room temperature orthorhombic structural phase there is a

significant volume contraction,[26] which influences the final lattice parameters taken up by the system dependant on the cooling route used.

Figure 1 shows the XRD peaks for both samples. The peaks of $CoMnSi_Q$ were considerably broadened compared to $CoMnSi_{SC}$, which could result from either grain size or strain (ε). Strain is most likely in this case, as both samples were prepared similarly, i.e. had the same powder/grain size. The significant change in the *a* lattice parameter is consistent with the statement that strain is dominant. The strain can be quantified by using:

$$\varepsilon = \frac{-\beta}{4\tan(\theta)} \qquad (4)$$

where ε is the strain, β is the ratio of the peak height to peak area, the integral breadth (equivalent to the full width half maximum, FWHM), and θ is the diffraction angle.[27] When the FWHM is plotted as a function of tan(θ) the strain in the material can be estimated from the gradient and it is clear from the inset in figure 1 that it is significantly larger in the quenched sample. From this analysis, ε was determined to be 1.36×10^{-3} for $CoMnSi_Q$ and 8.6×10^{-5} for $CoMnSi_{SC}$, the latter being at the limit of the instrument resolution.

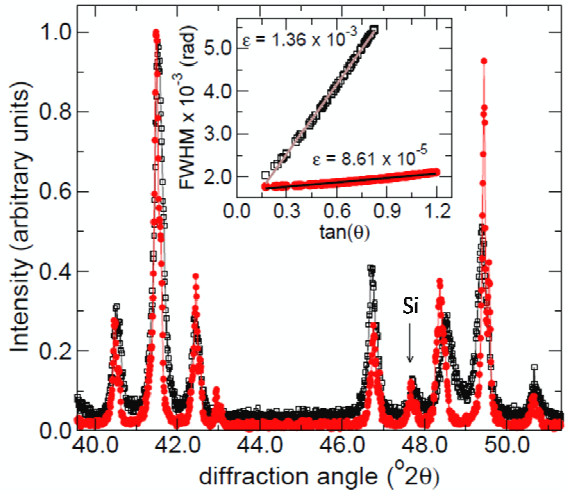

Figure 1. (Colour online) XRD of $CoMnSi_{SC}$ (solid circle) and $CoMnSi_{Q}$ (open square), showing broader peaks in the quenched sample. The intensity of the diffraction peaks has been normalized to 1 for comparison. An internal standard of Si was used in one of the scans and its contributing peak has been indicated by the black arrow. Inset shows the FWHM of Bragg peaks as a function of tan(θ), where θ is the diffraction angle.

3.2. Magnetization

The field and temperature dependence of the magnetic properties of $CoMnSi_{SC}$ and $CoMnSi_{Q}$ are summarized in figure 2. The insets show the isothermal entropy change calculated from the magnetization data using Eq. (3), for a field change of 0-2T and 0-5T. There are three significant differences between $CoMnSi_{Q}$ and $CoMnSi_{SC}$ that are evident from figure 2. Firstly, for a given field the AFM-FM transition temperature is lowered in $CoMnSi_{Q}$ by approximately 60K. Secondly, for the same critical field, H_c, the hysteresis of $CoMnSi_{SC}$ is about twice as large as that observed in $CoMnSi_{Q}$. For example, for H_c=5T, ΔH=0.33T in $CoMnSi_{Q}$ and 0.61T in $CoMnSi_{SC}$. Lastly, the M-H and M-T loops are broader in $CoMnSi_{Q}$ resulting is a lower ΔS_{peak} and a larger working temperature. It is interesting to note that a system with such broadened M-H loops still displays a small, but finite hysteresis.

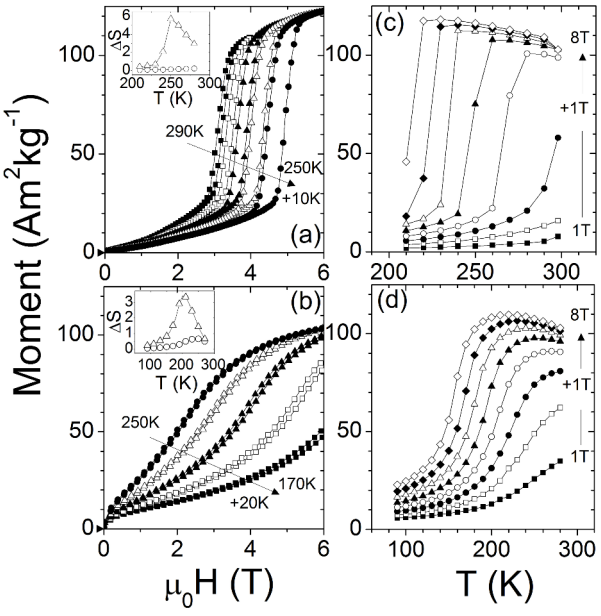

Figure 2. Isothermal *M-H* loops for a) $CoMnSi_{SC}$ at 10K intervals and b) $CoMnSi_{Q}$ at 20K intervals. Insets show the entropy change (in units of $JK^{-1}kg^{-1}$) calculated from this data using the Maxwell relation (Eq. 3) for field changes of 0-2T (open circle) and 0-5T (open triangle). Isofield *M-T* loops constructed from isothermal magnetization data in magnetic fields at 1T intervals between 1 and 8T for c) $CoMnSi_{SC}$ and d) $CoMnSi_{Q}$.

3.3. Microcalorimetry

The two samples were explored by taking small 100μm sized fragments and studying their properties using microcalorimetry. The heat capacity and latent heat were measured isothermally as a function of magnetic field at a series of temperatures and an example of the raw data obtained from these measurements is given in figure 3. Note that the error associated with microcalorimetry measurements is limited to the accurate determination of the sample mass, which was of the order of 5-10% but that the relative error is closer to 2%.

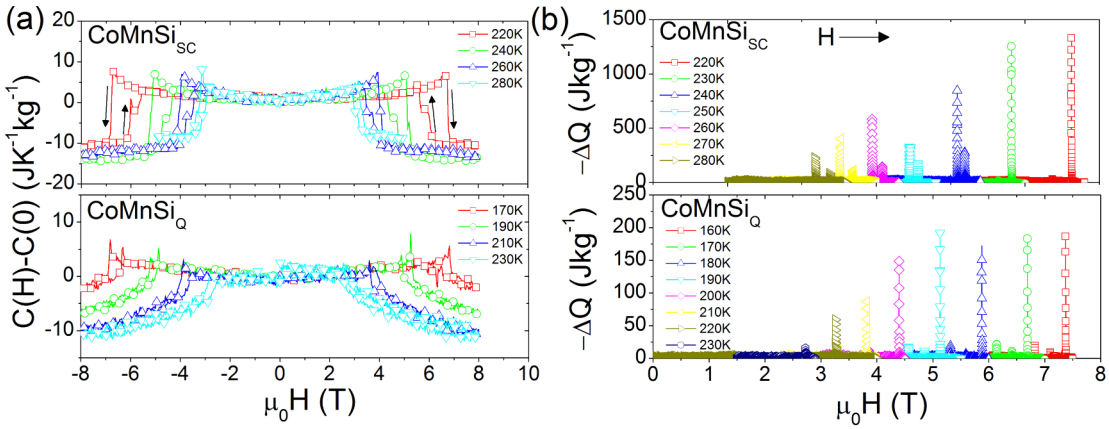

Figure 3. (Colour online) Comparison of raw data from a) heat capacity and b) latent heat measurements on $CoMnSi_{SC}$ and $CoMnSi_{Q}$. The heat capacity data is normalized to its zero field value for comparison of the relative changes at different temperatures.

Previous work has shown that $CoMnSi_{SC}$ undergoes a structural transition that couples with the magnetic one to produce notable ΔS,[16] even though the magnetic and structural entropy changes have opposite sign.[10] As the measured ΔS_{peak} determined from magnetisation (shown in figure 2) is much smaller in $CoMnSi_{Q}$ than in $CoMnSi_{SC}$ some difference in the latent heat might be expected and was observed in figure 3. The total entropy change of the ~$(100\mu m)^3$ sized fragment (sum of Eqs. (1) & (2)) and the bulk sample (Eq. (3)) are given in figure 4(a). The separate contributions to the entropy change calculated from heat capacity and latent heat measurements are shown in figure 4(b). Interestingly when the 60K shift in the transition temperature of $CoMnSi_{Q}$ with respect to $CoMnSi_{SC}$ is taken into account, the magnitude of the heat capacity contribution, ΔS_{HC} is similar for the two materials, whereas the latent heat measured in $CoMnSi_{Q}$ is approximately a factor of 4 smaller than that of $CoMnSi_{SC}$. Notice that for $CoMnSi_{SC}$ the bulk and fragment data agree well confirming sample homogeneity on the 100 μm scale. On the other hand, for $CoMnSi_{Q}$ there is a temperature offset of approximately 10K, indicating that the single fragment is not representative of the bulk, which suggests that the sample might be inhomogeneous. Indeed it is not clear if the reduced latent heat is due to a

material with uniformly depressed first order character or whether the material is inhomogeneous. In order to explore the latter possibility Hall probe imaging was used.

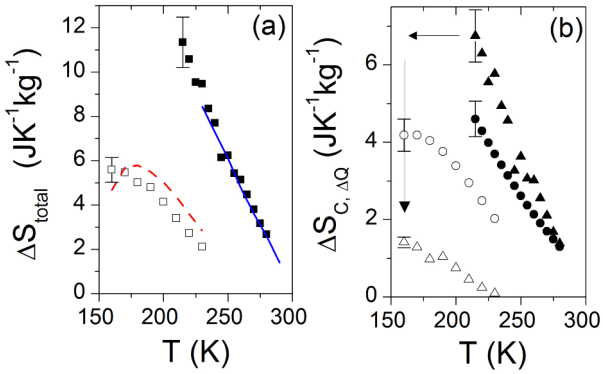

Figure 4. (Colour online) a) Total isothermal entropy change of $CoMnSi_{SC}$ (closed symbols) and $CoMnSi_{Q}$ (open symbols) for small fragments measured by calorimetry compared with ΔS_M derived from bulk magnetization measurements (-,---),b) Separate contributions to the entropy change, ΔS_{HC} (circles) & ΔS_{LH} (triangles), for $CoMnSi_{SC}$ (closed symbol) and $CoMnSi_{Q}$ (open symbol). The arrow indicates the reduction in latent heat at equivalent AFM-FM transition temperatures. All data in (a) & (b) is for a field change of 0-8T and the level of error is indicated by the error bars on the first data point (<10%).

3.4. Hall Probe Imaging

Figure 5 shows a selection of Hall probe images of the $CoMnSi_{SC}$ and $CoMnSi_{Q}$ samples across the magnetic field driven transition at 275 and 210K respectively. Notice that there is a clear nucleation and growth process present in figure 5(a) consistent with a first order transition and that it is accompanied by hysteresis in field (compare the images at the same absolute field for the up and downward sweep). The evolution of the latent heat associated with the magnetic transition in $CoMnSi_{SC}$ has been reported elsewhere,[22] also confirming that this sample exhibits a first order phase transition. In contrast figure 5(b) shows quite different properties in the $CoMnSi_{Q}$ sample, resembling classic second order behaviour: the moment increases continuously and there is no obvious widespread hysteresis.

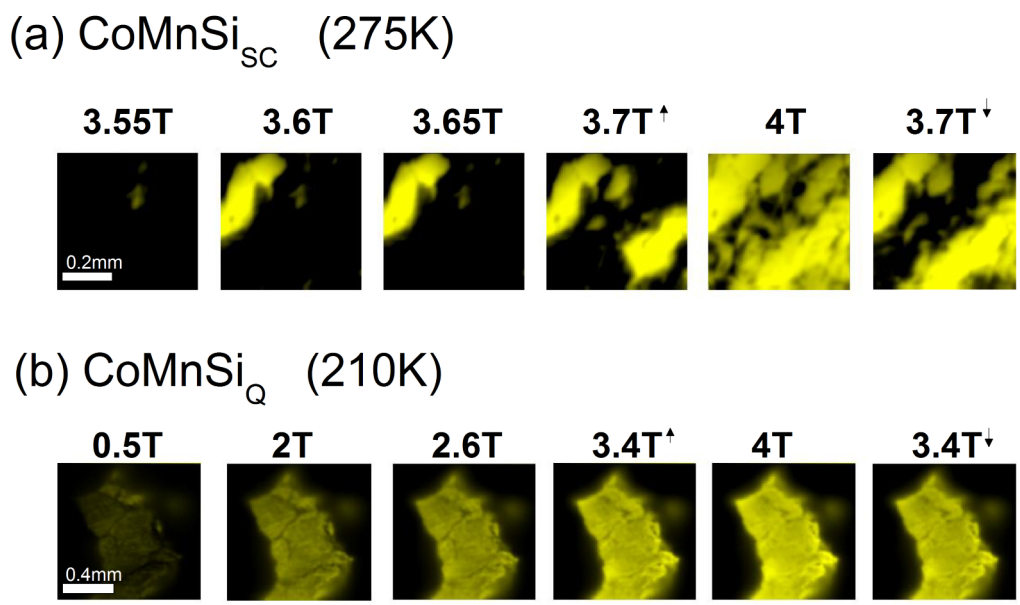

Figure 5. (Colour online) Hall probe imaging of a) $CoMnSi_{SC}$ at 275K and b) $CoMnSi_{Q}$ at 210K. The lengthscale has been indicated in the first image of each set and the colourscale is fixed as black for V_H=0 (AFM) and white (yellow online) for maximum V_H at 4T (FM). An additional image on the down-field sweep has been included to highlight any hysteresis. Note that $CoMnSi_{SC}$ shows clear first order behaviour with nucleation sites of the order of 100-200 micron.

In this system hysteresis can be linked to first order behaviour.[23] In order to highlight whether there is hysteresis in regions of the quenched sample, a series of images were taken at 210, 230, 250, and 290K in increasing and decreasing field between 0 and 4T. We then constructed what we call "difference images", by subtracting images taken at the same field value but opposite field sweep direction. At 290K the difference image was featureless indicating that the transition is reversible and without hysteresis, but for 210, 230 and 250K it was found that islands of hysteretic behaviour existed. These 'islands' also exhibited a range of critical fields, $H_c^{\uparrow,\downarrow}$, distributed across the phase transition, (where H_c is defined as the point at which M reaches 50% of its saturation value as the field was ramped up ($H_c^{\uparrow}$) and down ($H_c^{\downarrow}$)).

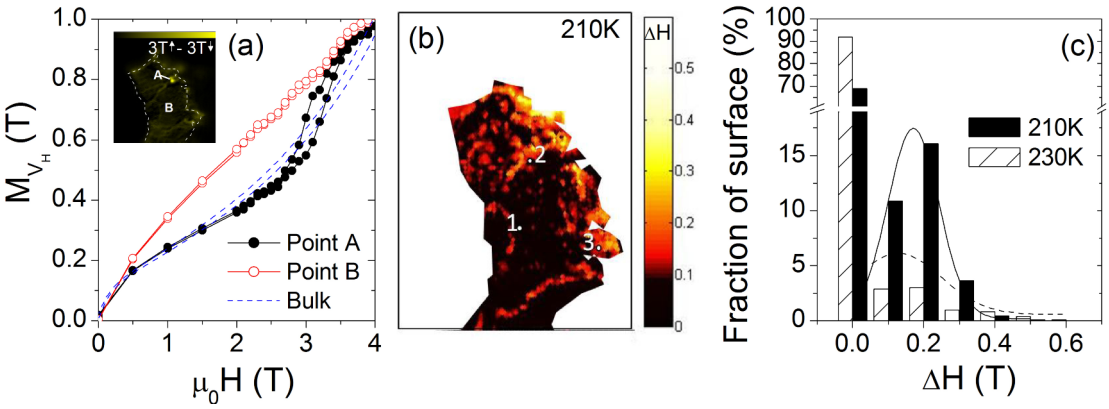

Figure 6. (Colour online) Hall probe imaging of $CoMnSi_Q$. a) Local *M-H* loops constructed from data taken for a single pixel at the two points marked A and B on the difference image (inset). The global *M-H* loop taken from the bulk sample at this temperature is also shown, normalized to M=1 at 4T, where the colour scale is fixed, with white (yellow online) corresponding to a large difference in moment, i.e. finite hysteresis, and black to zero or negligible difference in moment (ΔH=0). (b) Map of the hysteresis observed by Hall probe imaging at 210K. The colour scale indicates the magnitude of hysteresis where black (red online) for ΔH = 0 and white for ΔH>0.4. Points 1, 2 & 3 indicate areas that were investigated with EDX to check if there was some variation in stoichiometry associated with the change of magnetic behaviour. c) Statistical distribution of hysteresis, ΔH, measured for single pixels across the sample surface during Hall Probe imaging at 210 and 230K. A Gaussian fit for this data (ignoring ΔH =0) is indicated by the dotted and solid lines for 230 and 210K respectively.

The inset to figure 6(a) shows an example of a difference image, for $CoMnSi_Q$ at 210K. The image is shown on a fixed colour scale, so that the white (yellow online) area indicates that a sharp jump in moment from the AFM (black) to the FM (white) state occurred equivalent to hysteresis between the up-field and down-field sweeps. Region A is a brightly marked area with finite hysteresis. The local *M-H* loop (signal measured at a single pixel as a function of field) at the two points, labelled A & B, on the inset are plotted in figure 6(a). Note that the behaviour of these two points differs quite starkly. Point A exhibits hysteresis at a critical field of

approximately 3T indicating that a first order phase transition occurs. Point B, on the other hand increases smoothly and continuously in moment, indicative of a second order phase transition. We conclude that the material indeed appears to be magnetically inhomogeneous.

A colour map of the distribution of hysteresis across the sample surface at 210K is given in figure 6(b), which was constructed by determining the hysteresis of each pixel from local M-H loops. The statistical distribution of ΔH is summarized in the bar chart of figure 6(c) where the percentage of the surface that shows the given ΔH has been plotted. Aside from areas that show $\Delta H = 0$, at 210K and 230K there is a Gaussian distribution of ΔH values across the sample, as indicated by the fitted lines in the plot. As the images were taken at field intervals of 0.1T this represents the limit of the field resolution of ΔH. We comment that if strain is the controlling parameter tuning the magnetic behaviour, its distribution must also be inhomogeneous across the sample, resulting in the highly broadened XRD peaks.

The hysteresis observed by Hall probe imaging in $CoMnSi_Q$ varied across the sample surface as indicated by figures 6(b) and (c). To check that the variation in magnetic behaviour was not due to some local variation in stoichiometry, EDX was repeated on specific points on the sample surface chosen because these points exhibited varying degrees of hysteresis. It was found that there was no variation in the stoichiometry at the points marked 1 and 3 on figure 6(b). Similar analysis of $CoMnSi_{SC}$ showed the same atomic ratio as $CoMnSi_Q$.

Based on the statistical analysis in figure 6(c), it appears that at 210K ~ 70% of the sample surface exhibited second order behaviour, i.e. no hysteresis. At the higher temperature of 230K the fraction increases to 90%, as the effect of temperature on this system is to decouple the magneto-structural coupling.

4. Discussion

Hall probe imaging was used to show that the magnetic phase transition in $CoMnSi_Q$ has distributed magnetic properties that are either hysteretic (1^{st} order) or reversible (continuous). Calorimetry confirms the presence of latent heat in this sample albeit at a reduced magnitude (per unit mass) in comparison with $CoMnSi_{SC}$. The suppression of latent heat and the behaviour seen in Hall imaging suggests the sample is a spatially distributed mixture of 1^{st} and 2^{nd} order magnetic material occurring on a relatively fine scale (sub 100 micron).

From the Hall probe differential image map shown in figure 6(b) at 210K about 30% of the material, by area, appears to show hysteretic behaviour. We can reconstruct a bulk M-H loop, summing loops of type A and B shown previously in figure 6(a), weighed by the distribution suggested by Hall probe analysis. The reconstructed loop, shown in figure (7) agrees well with the observed bulk M-H loop at 210K, providing additional support for the mixed magnetic phase picture. The idea of a mixture is also supported by the reduction in measured latent heat in the $CoMnSi_Q$ fragment compared with the $CoMnSi_{SC}$ sample, as well as the apparent decrease in hysteresis. The quenching results in lattice contraction and compressive strain, producing a material, the majority of which (70% at 210K) shows second order-like transition properties, leaving small pockets of (presumably less strained) material with first order-like transition properties distributed throughout.

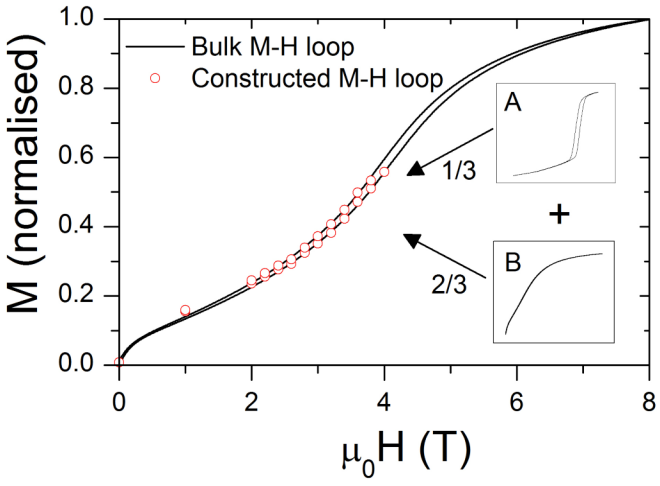

Figure 7 - Schematic of the *M-H* loop constructed from a combination of loops of type A and B (see figure 6(a)), in a weighting determined from Hall probe analysis (open circle) compared to the bulk M-H loop (solid line) at 210K. (See text for more details)

5. Refrigerant Capacity

The refrigerant capacity is used to compare the potential utility of different materials systems. A common approach is to calculate q from the full-width half-maximum (FWHM) area under the S(T) curve[3,4] where T_1 and T_2 in equation (5) are defined as the temperatures at which ΔS is half its maximum value, ΔS_{peak}. An additional measure suggested by Wood and Potter[28] is to select T_{hot} and T_{cold} so as to maximize equation (5) with $\Delta S(T_{hot}) = \Delta S(T_{cold})$ and $\Delta T = T_{hot} - T_{cold}$. We show the results of both calculations in figure 8, using expressions (5) and (6). Figure 7 demonstrates the areas over which these integrations were performed to calculate q_{FWHM} and q_{WP}.

$$q_{FWHM} = \int_{T1}^{T2} \Delta S(T)_H \, dT \qquad (5)$$

$$q_{WP} = \Delta S * \Delta T \qquad (6)$$

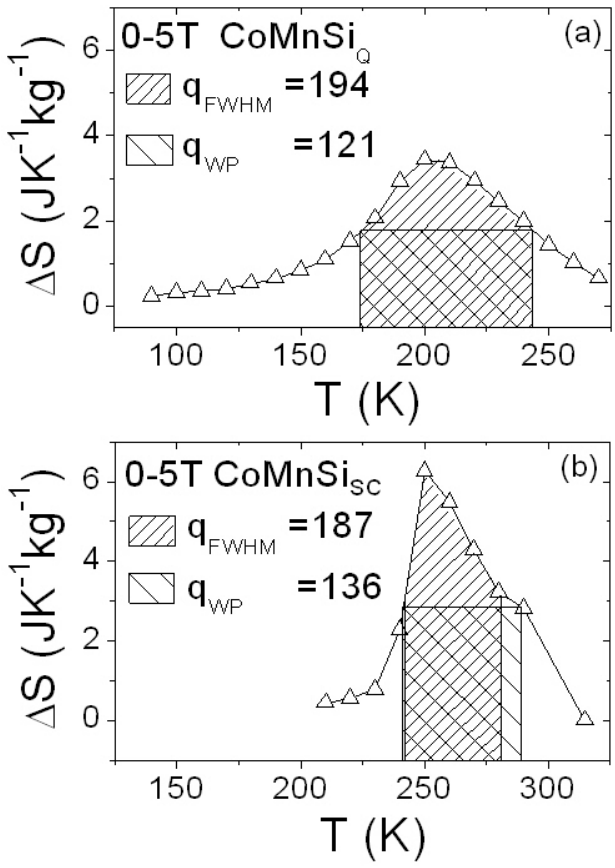

Figure 8. Refrigerant capacity calculated using the FWHM (dense shading) and Wood & Potter method (sparse shading) with a field change of 0-5T for a) $CoMnSi_Q$ and b) $CoMnSi_{SC}$.

Hysteresis loss also influences the effective refrigerant capacity, q_{eff}, and this can be determined by subtracting the energy loss due to hysteresis, E_{Hloss}, from q (see equations (7) & (8)). In Table 2 a summary of the hysteretic losses and refrigerant capacities calculated for both samples is shown. It is clear that E_{Hloss} of the $CoMnSi_Q$ sample is much smaller than in the slow cooled sample, but when this is subtracted from q_{WP} the result does not differ significantly between the two samples.

$$q_{eff} = q - E_{Hloss} \qquad (7)$$

$$E_{Hloss} = \oint M(H)dH \qquad (8)$$

Note that if the two systems are compared over the same temperature window, the refrigerant capacity is much greater for the single phase compound. For example, if we define a 50K temperature interval about ΔS_{peak} and integrate ΔS across this interal $q=149 Jkg^{-1}$ for $CoMnSi_Q$ and $218 Jkg^{-1}$ for $CoMnSi_{SC}$.

Overall, it appears that the use of magnetic phase mixtures presents some advantages, namely spreading the transition more widely with temperature and lowering the average hysteresis. We conclude that strain may be a useful tool to tune the magnetic properties to satisfy the specific requirements for any given application.

6. Conclusion

Different preparation techniques have been shown to produce a majority first or second order magnetocaloric effect. As expected the first order component gives larger ΔS_{peak} due to the extra contribution from latent heat, but by mixing first order and second order phase material we have shown that the impact on global magnetization is to broaden the transition in field and temperature and reduce the effective hysteresis. This reduction in hysteresis is a result of global averaging and not an improvement of caloric properties on a local atomic scale. The refrigerant capacity calculated using the two methods outlined here demonstrated that by manipulating the sample properties with the creation of magnetic phase mixtures, the useful temperature window can be enhanced whilst also retaining the materials' refrigerant capacity. The work demonstrates that magnetic phase mixtures offer a potentially interesting route to the engineering of materials that might produce improved overall properties for refrigeration applications.

Acknowledgments

This work was supported by EPSRC Platform grant EP/E016243/1 - A Platform to Develop and Utilize Characterization Tools for Functional Magnetic Materials. KGS would like to acknowledge S. Özcan and K. Roberts for help with sample preparation, G.G. Lonzarich for the use of sample synthesis facilities, and The Royal Society and the EPSRC Grant GR/R72235/01 for financial support.

TABLES:

Table 1. – XRD values of the $CoMnSi_{SC}$ and $CoMnSi_{Q}$ samples compared to measurements of the orthorhombic and hexagonal structural phase taken from [26]. The error on lattice parameters a, b & c is less than the lowest significant figure given.

Sample	**Preparation Route**	**a (**Å)	**b (**Å)	**c (**Å)	**V (**Å^3)
$CoMnSi_{SC}$	Annealed 60hours at 1223K, slow cooled at ~0.2K/min	5.867	3.685	6.851	148.2
$CoMnSi_{Ann}$	Annealed 60 hours at 1223K, quenched in water at RT	5.847	3.689	6.856	147.8
$CoMnSi_{(ORTH)}$[26]	Room Temperature	5.864	3.687	6.855	148.2
$CoMnSi_{(HEX)}$[26]	1273K	4.03	4.03	5.29	85.9

Table 2. Comparison of refrigerant capacity calculated using the Full Width Half Maximum method, q_{FWHM}, and the Wood & Potter method, q_{WP}, taking into account hysteretic losses, E_{Hloss}, for $CoMnSi_{Q}$ and $CoMnSi_{SC}$.

Sample	ΔS_{peak}	q_{FWHM}	q_{WP}	E_{Hloss}	q_{FWHM}- E_{Hloss}	q_{WP}- E_{Hloss}
	(JK^{-1}kg^{-1})	**(Jkg^{-1})**	**(Jkg^{-1})**	**(Jkg^{-1})**	**(Jkg^{-1})**	**(Jkg^{-1})**

$CoMnSi_{Q}$	3.5	194	121	9	185	112
$CoMnSi_{SC}$	6.3	187	136	27	160	109

[1] Tegus O, Brück E, Buschow KHJ & de Boer FR, 2002 *Nature* **415**, 150

[2] Pecharsky VK, Gschneidner, Jr KA, Pecharsky AO & Tishin AM, 2001 *Phys. Rev. B* **64**, 144406

[3]Pecharsky VK & Gschneidner, Jr. KA, 2001 *J. Appl. Phys*. **90**, 4614

[4] Sharma VK, Chattopadhyay MK & Roy SB, 2007 *J. Phys. D:Appl. Phys.* **40**, 1869-1873

[5] Provenzano V, Shapiro AJ & Shull RD, 2004 *Nature* **429**, 853-857

[6] Pecharsky VK & Gschneidner, Jr KA, 1997 .*Phys. Rev. Lett.* **78**, 004494

[7] de Campos A, Rocco DL, Carvalho AMG, Caron L, Coelho AA, Gama S, da Silva LM, Gandra FCG, dos Santos AO, Cardoso LP, von Ranke PJ & de Oliveira NA, 2006 *Nat. Mater. Lett.* **5**, 802-804

[8] Liu GJ, Sun JR, Lin J, Xie YW, Zhao TY, Zhang HW & Shen BG, 2006 *Appl. Phys. Lett.* **88**, 212505

[9]Jia L, Liu J, Sun JR, Zhang HW, Hu FX, Dong C, Rao GH and Shen BG, 2006 *J. Appl. Phys.* **100**, 123904

[10] Morrison K, Miyoshi Y, Moore JD, Barcza A, Sandeman KG, Caplin AD & Cohen LF, 2008 *Phys. Rev. B* **78**, 134418

[11] Gutfleisch O, Yan A & Müller KH, 2005 *J. Appl. Phys.* **97**, 10M305

[12] Gschneidner Jr, KA, Pecharsky VK, Tsokol AO, 2005 *Rep. Prog. Phys.* **68** 1479-1539

[13] Krenke T, Düman E, Acet M, Wasserman EF, Moya X, Mañosa L and Planes A, 2005 *Nat. Mat.* **4** 450.

[14] Nizioł S, Zach R, Senateur JP & Beille J, 1989 *J. Magn. Magn. Mater*. **79**, 333

[15] Nizioł S, Bińczycka H, Szytula A, Todorović J, Fruchart R, Senateur JP & Fruchart D, 1978 *Phys. Stat. Sol. (a)* **45**, 591

[16] Sandeman KG, Daou R, Özcan S, Durrell JH, Mathur ND & Fray DJ, 2006 *Phys. Rev. B* **74**, 224436

[17] Barcza A, Gercsi Z, Knight KS & Sandeman KG 2010, "Giant magneto-elastic coupling in a metallic helical metamagnet" *Preprint* cond-mat/1003.1206

[18] Katter M, Zellman V, Reppel GW & Uestuener K, 2009 "Magnetocaloric properties of reactively sintered $La(Fe,Co,Si)_{13}$" *Third International Conference on Magnetic Refrigeration at Room Temperature* (Des Moines, Iowa, USA), ed P W Egolf (Paris: International Institute of Refrigeration, Paris, 2009), pp. 83-88

[19] Zhang Q, Li WF, Sun NK, Du J, Li YB, Li C, Zhang YQ & Zhang, 2008 *J. Phys. D: Appl. Phys.* **41** 125001

[20] Moore JD, Perkins GK, Bugoslavsky YV, Cohen LF, Chattopadhyay MK, Roy SB, Chaddah P, Gschneidner KA & Pecharsky VK, 2006 *Phys. Rev. B* **73**, 144426

[21] Minakov AA, Roy SB, Bugoslavsky YV & Cohen LF, 2005 *Rev. Sci. Instr.* **76**, 043906

[22] Miyoshi Y, Morrison K, Moore JD, Caplin AD & Cohen LF, 2008 *Rev. Sci. Instr.* **79** 074901

[23] Morrison K, Moore JD, Sandeman KG, Caplin AD & Cohen LF, 2009 *Phys. Rev. B* **79**, 134408

[24] Tishin AM & Spichkin YI, 2003 *The Magnetocaloric Effect and its Applications*, Institute of Physics, Bristol

[25] Amaral JS & Amaral VS, 2009 *Appl. Phys. Lett.* **94**, 042506

[26] Johnson V, 1975 *Inorganic Chemistry* **14** 1117

[27] Snyder RL, Fiala J & Bunge HJ, 1999 "Defect and microstructure analysis by diffraction" International Union of crystallography monographs on crystallography, Oxford University Press, Oxford

[28] Wood ME & Potter WH, 1999 *Cryogenics* **25**, 667-683